Role of the PEWY Glutamate in Hydroquinone−Quinone Oxidation−Reduction Catalysis in the Q_o Site of Cytochrome bc_1†

Artur Osyczka,*,‡,|| Haibo Zhang,‡ Christelle Mathé,§ Peter R. Rich,§ Christopher C. Moser,‡ and P. Leslie Dutton‡

Johnson Research Foundation, Department of Biochemistry and Biophysics, University of Pennsylvania, Pennsylvania 19104, Glynn Laboratory of Bioenergetics, Department of Biology, University College London, Gower Street, London WC1E 6BT, U.K.

Received January 4, 2006; Revised Manuscript Received July 4, 2006

ABSTRACT: The glutamic acid residue of the conserved PEWY motif of the Q_o site of cytochrome bc_1 is widely discussed as central to reversible Q_o site catalysis of two-electron, two-proton hydroquinone−quinone oxidation−reduction. Extensive mutation of this glutamate (E295) to A, V, F, H, K, and Q in purple photosynthetic *Rhodobacter capsulatus* results in hydroquinone oxidation rates that are between 5 and 50-fold slower than that in the wild type. However, the mutants show little or no detectable effects on hydroquinone or quinone exchange and binding at the Q_o site nor on subsequent Q_o site-mediated redox equilibria in the c-chain and b-chain from pH 5−10. Lack of effects of mutations on the E_m/pH plots rules out involvement of E295 in the strong electron−proton coupling evident in either the FeS center or heme b_L. These detailed equilibrium and kinetic analyses demonstrate that E295 is not irreplaceable in the Q_o site catalytic mechanism. Rather, E295 and several other Q_o site residues that can also be widely varied and still support hydroquinone oxidation illustrate the considerable resilience of Q_o site activity to mutational change in Q_o site environs. Residues and water molecules appear to cooperate in providing a physical and chemical environment supporting hydroquinone oxidation rates comparable to those seen in nonprotein aqueous environments at electrodes. We suggest that residues at the Q_o site (and, possibly, other respiratory and photosynthetic quinone and oxygen binding sites) are a product of natural selection primarily acting not to lower catalytic barriers according to the traditional view of enzymatic catalysis but rather to develop specificity by raising barriers in defense of semiquinone loss or energy wasting short-circuit reactions.

The catalytic core of cytochrome bc_1, a common member of respiratory and photosynthetic chains, consists of two distinct electron transfer chains: the high-potential c-chain, normally including heme c_1 and the 2 iron-2 sulfur (FeS)[1] center, and the low-potential b-chain, normally including two hemes *b* and a quinone-binding Q_i site. These two chains meet at the quinone-binding Q_o site to reversibly double-oxidize hydroquinone in an unusual action that directs one electron into the c-chain and the other electron into the b-chain. The reaction at the Q_o site is initiated by the joint action of two flanking redox centers, the FeS center from the c-chain and the heme b_L from the b-chain. (See refs 1−4 (*1*−*4*) for recent reviews on cytochrome *bc* complexes.)

The energetic efficiency of cytochrome bc_1 requires that the Q_o site is engineered to ensure that the two electrons exchanged by oxidation of hydroquinone or reduction of quinone cannot both pass to or from just one chain. It follows that after this partitioning of the electrons into separate chains, single electrons must be prevented from moving directly from the low potential b-chain to the high potential c-chain, a reaction that is highly favored thermodynamically. There is still no useful mechanistic consensus on just how the Q_o site catalyzes hydroquinone/quinone oxidation/reduction and prevents such energy wasting short-circuit electron transfer reactions (*5*−*14*).

X-ray crystal structures of cytochrome *bc* complexes from a variety of sources have been presented over the past nine years (*15*−*21*). These structures have confirmed the expected close positioning of the electron-transfer cofactors within the c- and b-chains that promote electron tunneling typically in the tens of microseconds time range. They also revealed a large separation between the b-chain and the c-chain at the Q_o site; the distance across the site from the edge of heme b_L to the FeS center is 23 Å (Figure 1). This provides a simple way of slowing direct electron tunneling from the b-chain to c-chain (*5*, *6*). However, important structural details about the position of the quinone substrate within the Q_o site remain unavailable because Q_o site quinone has never been resolved in the X-ray structures. Inhibitors cocrystallized with cytochrome bc_1, such as stigmatellin, are often assumed

† This work was supported by U. S. Public Health Service Grant GM-27309 to P.L.D. and BBSRC Grant BB/C50747X/1 to P.R.R.

* To whom correspondence should be addressed. Phone: (48) 12-664-65-90. Fax: (48) 12-664-69-11. E-mail: osyczkaa@biotka.mol.uj.edu.pl.

‡ University of Pennsylvania.

§ University College London.

|| Current address: Faculty of Biochemistry, Biophysics and Biotechnology, Jagiellonian University, Gronostajowa 7, 30-387 Kraków, Poland.

[1] Abbreviations: FeS, 2 iron−2 sulfur; *Rba*., *Rhodobacter*; SDS−PAGE, sodium dodecyl sulfate-polyacrylamide gel electrophoresis; CW EPR, continuous wave electron paramagnetic resonance; ATR-FTIR, attenuated total reflection-Fourier transform infrared; Q, ubiquinone; QH_2, ubihydroquinone; E_m, redox midpoint potential; E_h, ambient redox potential; SHE, standard hydrogen electrode; K_i, concentration of inhibitor required to produce 50% inhibition; DPA, diphenylamine.

10.1021/bi060013a CCC: $33.50
Published on Web 08/11/2006

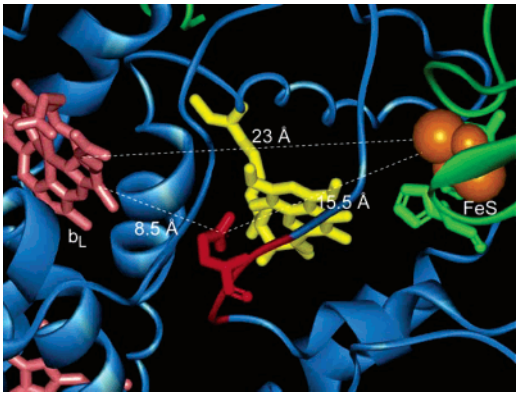

FIGURE 1: Close-up molecular view of the Q_o site from the crystal structure of *Rba. capsulatus* cytochrome bc_1 (*19*). The inhibitor, stigmatellin (yellow, stick), is in hydrogen-bond distances from Glu-295 (red stick) of the PEWY motif (red) of cytochrome *b* (blue ribbon) and from His-165 (green stick) of the FeS subunit (green ribbon).

to approximate the orientation of quinone when bound in the Q_o site and identify the amino acid side chains that interact with quinone in redox catalysis. If anything, the structures have amplified speculation about specific functional roles played by individual amino acids of the Q_o site.

Of these residues, the highly conserved PEWY loop of cytochrome *b* has received much attention, with Glu-295 (bacterial numbering)[2] assuming a central position in discussions of the Q_o site mechanism (*10*, *11*, *13*, *18*, *22*−*27*). Glu-295 gains notice as the only nearby protonatable carboxylic residue, although, intriguingly, it is replaced by nonprotonatable Val or Pro in certain bacteria (*1*, *28*, *29*). It is located between the FeS center and heme b_L, some 15.5 Å from the FeS center and 8.5 Å from heme b_L (Figure 1). Moreover, X-ray crystallography has shown that its side chain can adopt different orientations depending on the presence and type of Q_o site inhibitor used (*16*, *18*, *24*). The stigmatellin headgroup hydrogen-bonds to Glu-295 as well as one of the two His that ligate the FeS cluster (*12*, *18*). Mechanistic postulates for Glu-295 include a partnership with the His of the FeS cluster in binding quinone (*10*, *25*), proton release-binding coupled with heme b_L oxidation−reduction (*10*), critical involvement in the proton transfer as an essential proton donor/acceptor immediately interacting with the quinone bound in the Q_o site (*18*, *23*, *24*), and essential control in the movement of semiquinone intermediate through rotation of the Glu-295 side chain during its protonation/deprotonation (*13*, *22*).

A common view of catalysis is that there are a few key residues at a catalytic site, which individually provide essential chemical functions, such as electrostatic polarity, hydrogen-bond formation, and proton transfer, which by the process of natural selection have been carefully assigned unique roles and arranged in a special geometry that lowers the energy for the catalytic transition state and speed the reaction. The tool that is traditionally used to separate and identify these essential residues and their role in catalysis is site directed mutagenesis. This is usually done by using conservative mutations that maintain the size of a residue and, ideally, the structure of the site but change the residue's chemical function (e.g., proton transfer or hydrogen-bonding ability). When such substitutions have a large change in the catalytic rate, it is assumed that an essential residue has been found, and its chemical role has been identified.

However, this traditional interpretation of site directed mutagenesis tends to emphasize the role of that residue in isolation and diverts attention from the often dynamic and fundamentally cooperative nature of the roles of amino acids in enzyme function and energetics (*30*), a cooperativity that can obscure the quantitation of the contributions of specific residues to catalysis (*31*). Indeed, it is becoming increasingly apparent that catalytic sites can display a naturally selected resilience in which any one residue may be able to play an important role in catalysis by contributing chemical functions, such as polarity, hydrogen bonding, or proton transfer ability, but that the residue may not be essential because the dynamic nature of the catalytic site allows ready replacement of these functions by other residues and mobile water molecules when the residue in question is changed. Catalytically resilient sites will tend to be favored during the random mutational insults of evolution. Clearly, when site-directed mutation causes dramatic 10^4 to 10^6 changes in catalytic rates, these residues earn the description of essential (*31*, *32*). However, with rate changes of 4−7, which have been described as relatively small (*33*), the interpretation of residue significance is more problematic. The 2 to 50-fold mutagenic rate changes for Glu-295 (*22*, *34*−*36*) are in this problematic range and have stimulated a confusing range of interpretations.

To examine the role of Glu-295, we have extended the existing data in the literature to broadly characterize a family of Q_o site mutants of Glu-295 in photosynthetic purple bacterium *Rhodobacter* (*Rba.*) *capsulatus*. We have conducted a detailed examination of the effects that these substitutions have on equilibrium properties, hydroquinone−quinone exchange and binding affinities, changes in reaction driving force, and a possible role of Glu-295 in governing the redox equilibrium and the time scale of Q_o site catalysis. We find that Glu-295 has little or no detectable contribution to substrate binding and redox equilibria in the site; neither does it appear to play an irreplaceable mechanistic role in partnership with the FeS center or heme b_L or in proton management by the Q_o site. We find that Glu-295 joins several other residues within the Q_o site, where hydroquinone−quinone oxidation−reduction catalysis displays considerable resilience to mutational change. We propose that Glu-295 may be part of a consortium that cooperates in establishing a simple polar environment sufficient to promote hydroquinone−quinone oxidation and reduction at rates that are not very different from uncatalyzed rates of oxidation and reduction by electrodes in water (*37*−*39*).

MATERIALS AND METHODS

Preparation of Mutated Cytochrome bc_1 Complexes. Rba. capsulatus strains with mutated cytochrome bc_1 were generated as described previously (*40*). The mutations were constructed by site directed mutagenesis using the QuikChange system from Stratagene and the plasmid pPET1 (a derivative of pBR322 containing a wild-type copy of *petABC*) as the template DNA. After sequencing, the appropriate DNA fragments bearing the desired mutation and no other mutations were exchanged with their wild-type counterparts in

[2] This corresponds to Glu-272 in mitochondrial cytochrome bc_1 and Glu-78 in plant cytochrome b_6f.

pMTS1 (the expression vector containing a copy of *petABC* and a kanamycin resistance cartridge (*41*)) using the restriction enzymes *Sfu*I and *Xma*I. The mutated variants of pMTS1 were then introduced into the MT-RBC1 strain (*petABC*-operon deletion background (*40*)) via triparental crosses as described previously (*40*). The presence of engineered mutations was confirmed by sequencing the plasmid DNA isolated from the mutated *Rba. capsulatus* strains.

Optical and EPR Analyses. Chromatophore membranes and purified cytochrome bc_1 complexes were prepared as described in refs 40 and 41 (*40*, *41*). SDS−PAGE was performed according to Laemmli using a 15% linear separating gel as described in ref 42 (*42*). Optical spectra were recorded on Perkin-Elmer UV/Vis spectrophotometer (Lambda 20) fitted with an anaerobic redox cuvette when necessary. Chemical oxidation−reduction midpoint potential titrations of hemes *b* in chromatophores were performed as described in ref 43 (*43*). The titrations were performed in 50 mM Citrate (for pH 5.1), 50 mM MES (for pH 6.0), 50 mM MOPS (for pH 7.0), 50 mM Tris (for pH 8.0 and 9.0), 50 mM CAPS (for pH 10.0) containing 100 mM KCl and redox mediators 2,3,5,6-tetramethyl-1,4-phenylenediamine, 1,2-naphthoquinone-4-sulfonate, 1,2-naphthoquinone, phenazine ethosulfate, phenazine methosulfate, duroquinone, pyocyanine, 2-hydroxy-1,4-naphthoquinone, anthraquinone-2-sulfonate, and benzyl viologen, at concentrations of 15−30 μM. The optical changes that accompanied the redox potential change were recorded in the α-band region (500−600 nm), and the E_m values were determined by fitting the 560−540 nm difference to the Nernst equation for two one-electron couples.

CW EPR measurements were performed on a Brucker ESP300E spectrometer with temperature control maintained by an Oxford ESR 900 continuous-flow liquid helium cryostat interfaced with an Oxford ITC4 temperature controller. The frequency was measured by a Hewlett-Packard 5350B frequency counter. The EPR parameters were sample temperature, 20 K; microwave frequency, 9.447 GHz; microwave power, 2 mW; modulation frequency, 100 kHz; modulation amplitude, 20.0 G; and time constant, 164 ms.

Potentiometric titrations of the FeS center in chromatophores were performed in 50 mM MOPS at pH 7.0, containing 100 mM KCl and mediators 2,3,5,6-tetramethyl-1,4-phenylenediamine, 1,2-naphthoquinone-4-sulfonate, 1,2-naphthoquinone, 2,3,5,6-tetrachlorohyroquinone, and 1,4-benzoquinone, each at a concentration of 100 μM. At each potential, the fraction of the reduced FeS center was determined from the amplitude of the g_y signal of the EPR spectrum, and the data were fit to the Nernst equation for a one-electron couple.

Redox titrations of the g_x transition of the EPR of the FeS center in chromatophores were performed in 50 mM MOPS at pH 7.0, containing 100 mM KCl and mediators 2,3,5,6-tetramethyl-1,4-phenylenediamine, 1,2-naphthoquinone-4-sulfonate, 1,2-naphthoquinone, phenazine ethosulfate, phenazine methosulfate, duroquinone, pyocyanine, and 2-hydroxy-1,4-naphthoquinone, each at a concentration of 50 μM. Normalized g_x amplitudes at 1.80 were fit to the Nernst equation for a two-electron couple.

FTIR Analysis

Film Preparation. Production of stable films for ATR-FTIR measurements required the depletion of detergent so that the sample became sufficiently hydrophobic. Film preparation and rehydration on a silicon microprism (3 mm diameter, three-bounce, SensIR Europe) were essentially the same as that described previously (*44*, *45*). Stock cytochrome bc_1 (20−40 μM) (10−20 μL) was diluted into 3 mL of 20 mM potassium phosphate buffer (pH 7.5) containing 0.015% (w/v) sodium cholate and 0.015% (w/v) octyl glucoside and pelleted by centrifugation. The pellet was washed twice with the same buffer, and once with 1mM potassium phosphate buffer (pH 7.5) to form ATR-ready material, which was dispersed into 10 μL of distilled water and stored if necessary at −80 °C. Films were formed by drying of 2 μL of ATR-ready material and 4 μL of distilled water onto the prism followed by rehydration with 200 μL of 50 mM potassium phosphate and 100 mM potassium chloride at pH 7.5.

Redox Cycling and Data Acquisition. All potentials are quoted versus that of the standard hydrogen electrode. Automated cycling between reduced and oxidized states was achieved with an in-house constructed electrochemical cell operating in conventional three-electrode mode (*46*). The potential between working and reference electrodes was set with a Model 704 PAR potentiostat and modulated with a computer-controlled offset device. The working electrode was a 9 mm glassy carbon disk, cleaned before use with a paste of 0.03 mm alumina powder, which formed the top of a sample chamber of less than 0.3 mm thickness. The auxiliary electrode was a platinum sheet (40 mm^2 surface area) connected to the sample by a porous glass frit, and a Ag/AgCl reference electrode provided a reference voltage of + 204 mV versus SHE. Redox mediation between the glassy carbon electrode and protein film was provided by a buffer of 20 mM potassium phosphate, 100 mM potassium chloride at pH 7.5 and with 25 μM benzyl viologen (E_{m7} = −350 mV), 50 μM anthraquinone-2,6-disulfonate (E_{m7} = −185 mV), and 50 μM gallocyanin (E_{m7} = + 20 mV). For redox difference spectra of heme b_L, the applied potential was alternated between −340 and 0 mV, and 10 min was allowed for equilibration.

IR spectra were recorded with a Bruker IFS 66S spectrometer fitted with a liquid nitrogen-cooled MCT-B detector. All frequencies quoted are accurate to ± 1 cm^{-1}. Typically, the reduced minus oxidized difference spectra shown consisted of data averaged from 50 oxidative and 50 reductive cycles, with individual spectra computed from 1000 interferograms at 4 cm^{-1} resolution. Where necessary, baseline corrections due to protein swelling/shrinkage and contributions from mediators and buffer were removed by interactive subtraction.

Flash-Induced Electron Transfer Measurements

Flash-activated turnover kinetics of cytochrome bc_1 were performed essentially as described in refs 47 and 48 (*47*, *48*) on a double wavelength spectrophotometer (Biomedical Instrumentation Group, University of Pennsylvania). Chromatophore membranes were suspended in the appropriate buffer (the buffers used for each pH were the same as those used in the redox titrations) and redox poised in the presence of 2.5 μM valinomycin and redox mediators 2,3,5,6-

tetramethyl-1,4-phenylenediamine, 1,2-naphthoquinone, and 2-hydroxy-1,4-naphthoquinone, each at a concentration of 8 μM, and phenazine ethosulfate and phenazine methosulfate at concentration of 1 μM, and 60 μM benzyl viologen. The quantity of chromatophore membranes used in the assays corresponded to the 0.2−0.35 μM reaction center, whose concentration was determined from the flash-activated absorbance change of the bacteriochlorophyll dimer oxidation at 602−540 nm in a sample poised at 380 mV and using an extinction coefficient of 29.8 mM^{-1} cm^{-1} (*47*, *48*). Transient cytochrome *b* reduction kinetics initiated by a short saturating flash (8 μs) from a xenon lamp were followed at 560−570 nm. Inhibitors antimycin A, myxothiazol, and stigmatellin were used at concentrations of 5, 5, and 1 μM, respectively.

RESULTS

General Properties of Glu-295 Mutants. The family of Glu-295 mutants generated in *Rba. capsulatus* includes side chain replacements to both polar and nonpolar groups of various bulkiness (Ala, Val, Gln, Phe) as well as side chains oppositely charged when protonated and with p*K* values several units higher than that of the carboxyl of glutamate (Lys and His). For each mutant, cell strains showed a photosynthetically competent (Ps^+) phenotype with similar growth rates as that of the wild type, indicating that mutated cytochromes bc_1 assemble correctly and are functional *in vivo*. Cytochrome bc_1 purified from the membranes of mutated strains (E295V and E295H) displayed typical wild-type optical difference spectra and subunit composition on SDS−PAGE gels (not shown), indicating that Glu-295 mutations did not affect the overall structure and stability of the complex in its isolated form.

Testing Glu-295 Partnership with the FeS Cluster in Binding Q/QH_2 and Inhibitors, and in Controlling FeS Cluster Redox Potentials. If Glu-295 and FeS cluster-ligated histidine are critical anchors for quinone binding, mutating these anchors may generally weaken quinone binding, or there may be a differential change in reduced versus oxidized quinone binding affinity. This could lead to observable changes in the paramagnetic reduced FeS cluster EPR spectra and/or E_m values when the glutamate is mutated. Progressive quinone extraction of chromatophore membranes indicates a binding constant for quinone at the Q_o site equivalent to a ratio of between 1 and 3 quinones per cytochrome bc_1, about 5% of the full quinone pool complement, with approximately equal binding affinities for oxidized and reduced quinones (*49*). Ignoring possible compensating effects in a mutant protein, the loss of a hydrogen bond should reduce the binding affinity by 1−2 kcal/mol or about an order of magnitude, leading to a predicted occupancy of the quinone site of approximately 2/3 in unextracted membranes, which should in principle be detectable by EPR spectroscopy. Figure 2A provides information on the interaction of FeS with oxidized Q in the Q_o site in chromatophore membranes from both wild-type and mutant strains. In the absence of any other treatments, as is the case here, a characteristic sharp g_x transition close to 1.800 commonly signals FeS interacting with a Q_o site fully occupied by Q from the oxidized Q pool. This transition shifts to 1.783 when the Q pool is partially extracted or to 1.765 when fully extracted (*49*, *50*). The FeS cluster spectrum of the wild type is typical of a fully occupied Q_o site. The Glu-295 mutants Val, Ala, Phe and Gln, which

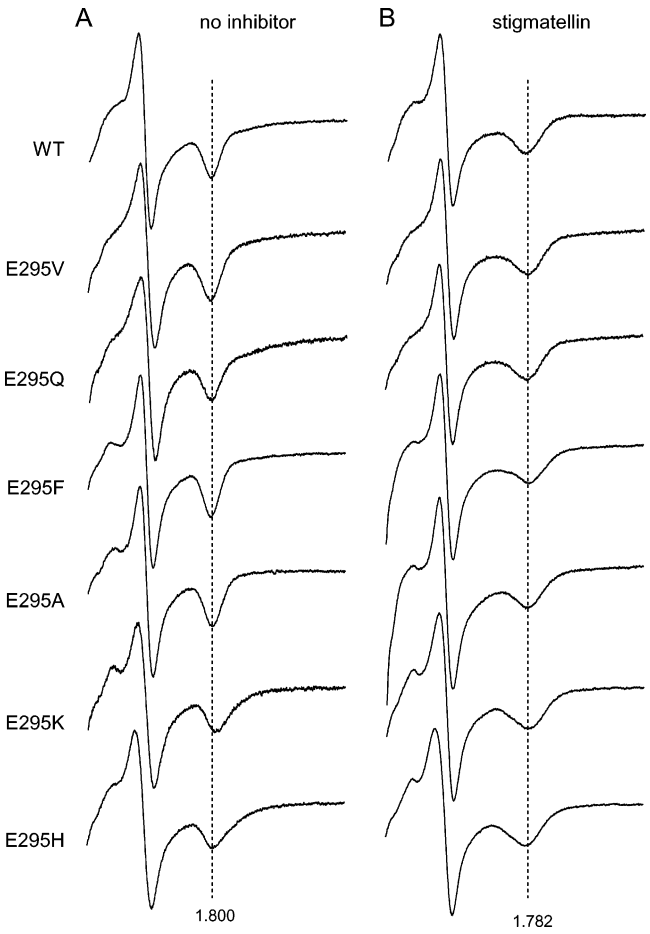

FIGURE 2: EPR spectra showing g_y and g_x features of the FeS center in the wild type and in Glu-295 mutants. Chromatophores were suspended in 50 mM MOPS and 100 mM KCl at pH 7 at a 20−30 μM concentration of cytochrome bc_1. Samples were reduced with ascorbate in the absence of any inhibitor (A) or in the presence of stigmatellin (B).

offer a simple avenue to examine the loss of the carboxyl group against the gain of an aliphatic, aromatic, or amide group, show no detectable differences in the FeS cluster spectra. Although it is conceivable that Q still interacts with FeS in these mutants but that both are displaced from the Q_o site, the simplest conclusion is that the loss of the carboxyl group of Glu-295 has no observable effect on Q_o site occupancy. However, replacing acidic Glu with more basic His causes a slight broadening of g_x transition suggesting weakened binding, whereas replacing Glu with the much more basic Lys induces a small shift to lower g-values (g_x 1.792) indicating weakened affinity or, possibly, a rearrangement of residues in the quinone/FeS environment, as seen before in the F144K mutant (*51*).

Figure 2B shows an analogous series of measurements after the addition of a slight stoichiometric excess of the high affinity inhibitor stigmatellin, seen in X-ray crystal structures to interact directly with both His-161 of the FeS subunit and Glu-295 of cytochrome *b* (*12*, *18*). The Figure compares the wild-type spectrum with its characteristic g_x transition close to 1.782 with those of the mutants. In all mutants, the addition of stigmatellin results in the same characteristic shift of g_x to 1.782. This indicates that the loss of the carboxyl group on Glu-295 and the gain of an aliphatic, aromatic, basic, or amide side chains does not detectably alter the response of the FeS cluster to the presence of the inhibitor.

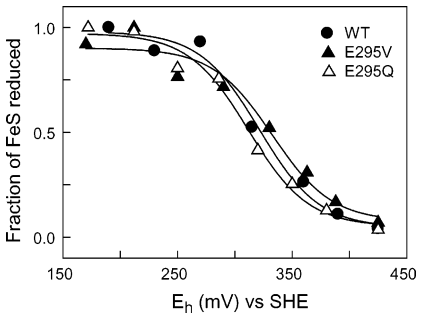

FIGURE 3: Dark redox equilibrium potentiometric titration of the FeS cluster of cytochrome bc_1 in the wild type and mutants E295V and E295Q. Titrations were performed in chromatophores in 50 mM MOPS and 100 mM KCl at pH 7. Normalized amplitudes of the g_y signal in wild type (●), E295V (▲), and E295Q (△) fit to an $n = 1$ Nernst equation. The E_{m7} values obtained from the fitting are 320 mV (for wild type), 332 mV (for E295V), and 312 mV (for E295Q).

However limitations to quantifying the effects of mutation on the Q_o site affinity for the inhibitor are more stringent than that for quinone affinity because the concentrations of cytochrome bc_1 used for EPR (30 μM) are much greater than the K_d (<nM) value for stigmatellin (*52*, *53*). This restricts measurement to effects of greater than several orders of magnitude of the weakening of inhibitor binding; we note that kinetic measurements performed at 0.15 μM cytochrome bc_1 (such as those of Figures 9 and 10) still failed to reveal the weakening effects in Glu-295 mutants to the addition of 1 μM stigmatellin.

It is well known that the FeS redox potential can change when inhibitors are bound to the Q_o site. Stigmatellin causes a substantial rise in the FeS E_m value of 250 mV (*54*), *ortho*-hydroxyquinone analogues raise E_m by 45−70 mV (*55*, *56*), and even inhibitors such as myxothiazol and diphenylamine, which interact with the heme b_L side of the Q_o site, shift the FeS potential by about 30 mV down and up, respectively (*57*−*59*). Moreover, the FeS redox potential has been reported to change when mutations that restrict the motion of the FeS head domain are introduced (*57*, *60*, *61*), and/or the Q pool is chemically depleted of quinone (*62*). Yet, as shown in Figure 3 for the E295V and E295Q mutants, the removal of the carboxyl and the loss of a hypothetical hydrogen-bond possibility to quinone has no detectable effect on the redox midpoint potential of the FeS cluster at pH 7.0. This indicates that the carboxyl group of Glu-295 and putative H-bonding to a bound quinone in the Q_o site plays little or no role in controlling the E_m value of the FeS cluster.

Quinone and hydroquinone from the quinone pool bind at the Q_o site with about equal affinity, as shown by the similar redox midpoint potential of quinone in the Q_o site and in the pool (*49*). If deprotonated Glu-295 is energetically important in hydrogen bonding and binding to the reduced hydroquinone hydroxyl (a hydrogen bond that cannot be made to oxidized quinone), then removing this hydrogen bond by mutation may be expected to change the relative affinity of oxidized and reduced quinone for the site, resulting in a change in the quinone midpoint potential. This can be tested by monitoring the Q-pool sensitive g_x transition of the EPR spectrum of the FeS center; the line shape changes from a narrow $g = 1.80$ trough when the Q pool is oxidized to a broader $g = 1.77$ trough when the Q pool is reduced (ref 49 (*49*) and Figure 4A). Redox titrations of the EPR g_x transition show no noticeable change in the redox midpoint potential of Q_o site quinone when Glu-295 is replaced by the nonhydrogen-bonding Val or when the potentially hydrogen-bond-accepting $-COO^-$ group of Glu is replaced with $-NH_2$ in Gln (Figure 4B). This suggests three possibilities: redox state sensitive hydrogen bonding of Glu to

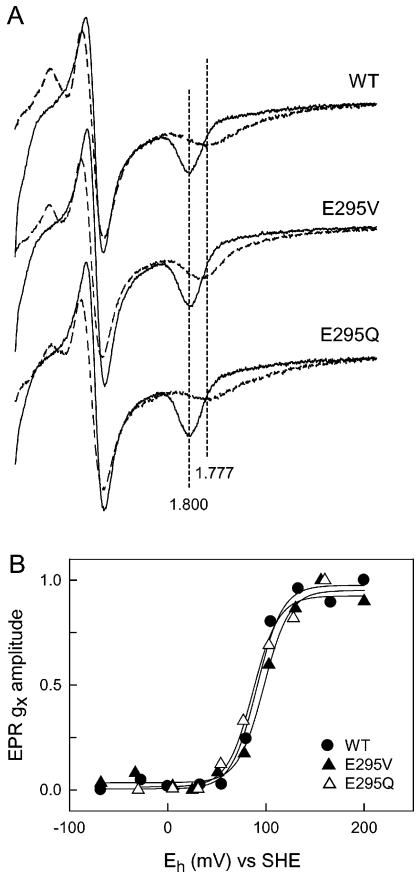

FIGURE 4: Dark redox equilibrium potentiometric titration of the EPR g_x transition of the FeS cluster in the wild type and mutants E295V and E295Q. Titrations were performed in chromatophores in 50 mM MOPS and 100 mM KCl at pH 7. (A) EPR spectra at $E_h = +170$ mV poising the Q-pool oxidized (—) and at $E_h = -40$ mV poising the Q-pool reduced (---). (B) Normalized g_x amplitudes at 1.80 in the wild type (●), E295V (▲), and E295Q (△) fit to an $n = 2$ Nernst equation. The E_{m7} values for the Q_o site quinone obtained from the fitting are 91 mV (for wild type), 98 mV (for E295V), and 87 mV (for E295Q).

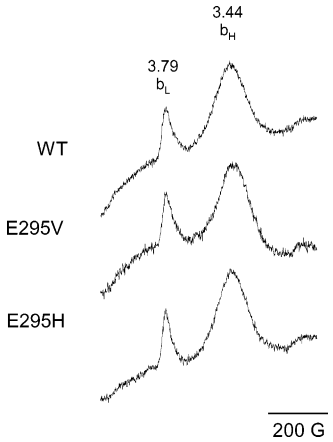

FIGURE 5: EPR spectra of hemes b_L and b_H of wild-type cytochrome bc_1 and mutants E295V and E295H. Isolated cytochrome bc_1 complexes were reduced with ascorbate. EPR conditions are described in Materials and Methods.

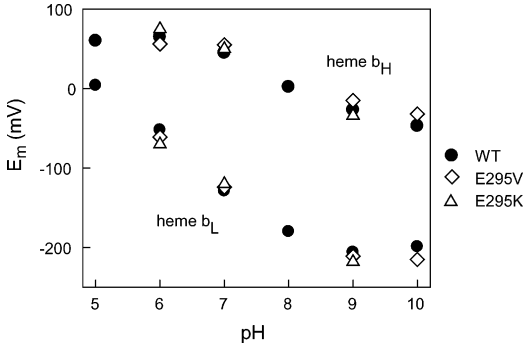

FIGURE 6: pH dependence of hemes b_L and b_H equilibrium redox midpoint potentials in cytochrome bc_1 of the wild type (●) and mutants E295V (◇) and E295K (△).

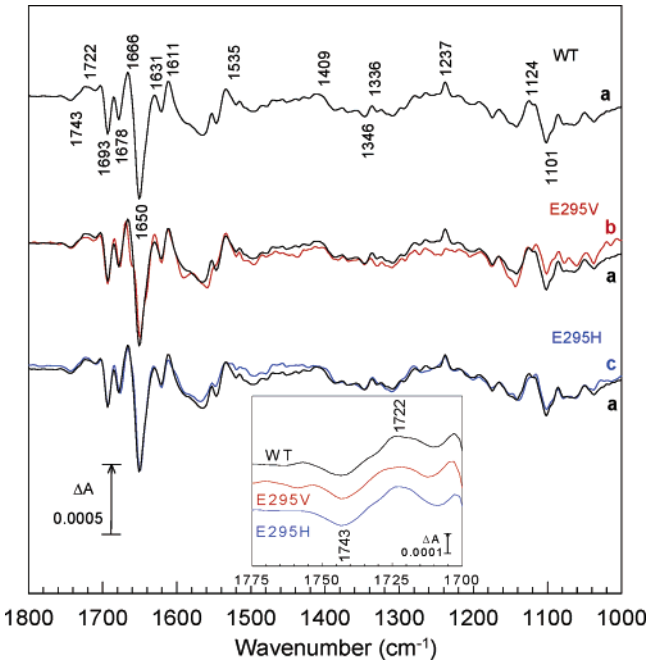

FIGURE 7: Electrochemically induced reduced minus oxidized ATR-FTIR difference spectra of heme b_L of cytochrome bc_1 in the wild type and mutants E295V and E295H. Data were obtained as described in Materials and Methods. Trace a (black), wild type; trace b (red), mutant E295H; trace c (blue), mutant E295V. The wild-type data of trace a are redrawn over the mutant data for purposes of comparison. The inset shows an expansion of the 1775−1700 cm^{-1} region of traces a−c.

quinone is energetically relatively unimportant or that Glu contributes an exactly balanced energetic contribution as a hydrogen-bond donor for oxidized quinone and a hydrogen-bond acceptor for reduced quinone, or, as seems more likely, other residues or water molecules besides Glu provide quinone-binding hydrogen bonds.

Testing Glu-295 Interaction with Heme b_L for Proton Coupling to Heme Oxidation/Reduction. Heme b_L in bacterial cytochrome bc_1 displays a conspicuous pH dependency with oxidized and reduced p*K* values of unknown origin at <5 and 9 (*5*). Glu-295 could be a reasonable candidate for the protonation site and might even be part of a heme b_L redox state sensitive double-gating mechanism that controls quinone/hydroquinone binding or electron-transfer energetics proposed to prevent short circuits (*5*, *6*, *10*). If there is strong and functionally important structural or electrostatic coupling between the protonation of Glu-295 and the redox behavior of heme b_L, then its removal might be accompanied by

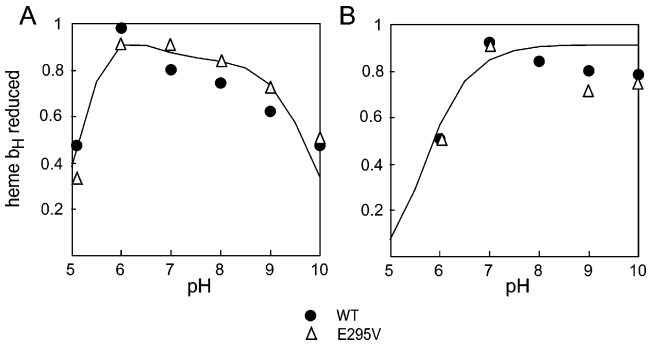

FIGURE 8: Extent of flash-activated Q_o site catalysis in wild-type cytochrome bc_1 and E295V mutant. Heme *b* reduction yields (wild type (●); E295V (△)) were recorded in the presence of antimycin with the Q-pool half-reduced (A) or the Q-pool oxidized. (B). The line traces the extent of reduction expected on the basis of a Q_o site-mediated quasi-equilibrium between the high and low potential chains using equilibrium redox midpoint determinations (*5*).

observable changes in the EPR spectra of the paramagnetic ferric heme b_L or, more likely, by changes in heme b_L E_m and p*K* values and in FTIR redox spectral transitions.

Figure 5 compares the EPR spectra of oxidized hemes *b* of cytochrome bc_1 isolated from the wild type and E295V and E295H mutants. Characteristically shaped peaks with maxima at g_z 3.79 for heme b_L and at g_z 3.44 for heme b_H (*63*) are evident in both mutants and in the wild type. Thus, the EPR spectra of the hemes *b* of the mutants show no signs of Glu-295 influence on the environment of heme b_L or the more distant heme b_H. This contrasts with mutations closer to heme b_L, such as G146A or G146V, that significantly change the shape of the EPR spectrum of ferric heme b_L (*64*). Even distant Q_i site inhibitors such as antimycin affect heme b_L EPR spectra more than Glu-295 mutants (*65*, *66*).

Figure 6 compares the E_m/pH profile of heme *b* components of the wild type with those of E295V and E295K mutants. Clearly, the mutations change neither E_m values nor p*K* values of the hemes *b*. This indicates that the carboxyl group of Glu-295 is not responsible for strong proton coupling that leads to a pH dependence of heme b_L. Further, the similar lack of effect on the E_m/pH profile of heme b_H provides no support for long range effects from Glu-295 on heme b_H.

To more closely search for spectroscopic signatures of acid−base transitions that accompany heme b_L oxidation−reduction, we have examined the redox difference FTIR spectra of purified cytochrome bc_1 complexes (Figure 7). The spectra are dominated by amide I and II polypeptide backbone changes and redox-sensitive bis-histidine-heme modes but also contain changes that arise from specific amino acids. Particularly relevant to the present study is a peak/trough at 1722/1743 cm^{-1}, frequencies that are characteristic of protonated carboxylic acids (Figure 7, inset) (*67*, *68*). In the heme b_L spectra here, the change consists of an overlapping peak/trough, indicating that the change most likely arises from the environmental changes of a single, protonated carboxylic residue or, possibly, the redistribution of protons between several carboxylic residues. In any case, the FTIR spectra accompanying heme b_L oxidation/reduction in mutants E295V and E295H reveal no significant changes in the 2000−1000 cm^{-1} range (Figure 7). Thus, although a clear signature of carboxylic acids that are coupled to heme b_L oxidation/reduction is present, the present data appear to

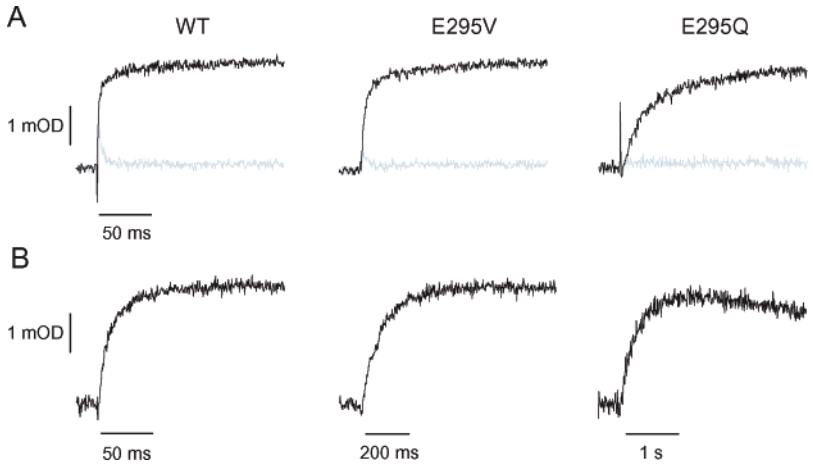

FIGURE 9: Flash-activated heme *b* reduction in the wild type and mutants E295V and E295Q. Kinetic transients at 560−570 nm were recorded at pH 7 with the Q-pool half-reduced (A) or the Q-pool oxidized (B) in the presence of antimycin (black traces) or in the absence of any inhibitors (grey traces).

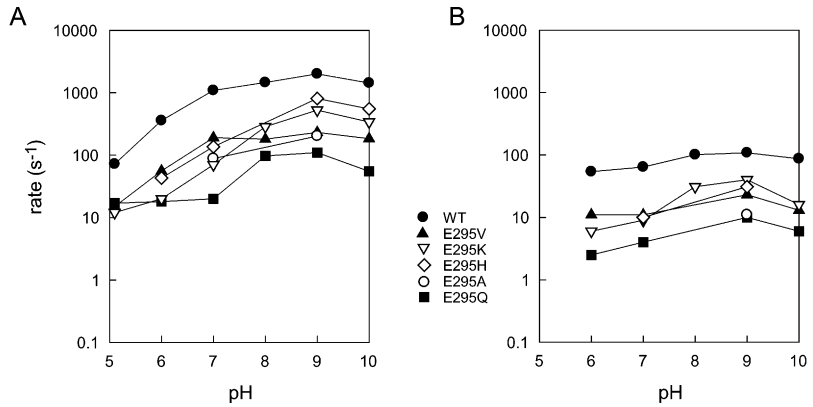

FIGURE 10: Rates of flash-activated heme *b* reduction in the wild type and Glu-295 mutants. Rates for the wild type (●), E295V (▲), E295K (▽), E295H (◇), E295A (○), and E295Q (■) were obtained from the exponential fits of the experimental traces recorded in the presence of antimycin with the Q-pool half reduced (A) or the Q-pool oxidized (B).

rule out an involvement of Glu-295 and point instead to the heme propionates or other nearby carboxylic acids.

Testing the Effect of Glu-295 in Governing the Q Pool and c- and b-Chain Redox Equilibria. Using antimycin to completely knock out Q_i site activity and prevent electron transfer out of the b-chain sets up a sensitive test for the role of Glu-295 in modulating the redox potentials of any component in the b- and c-chains and Q_o site during catalysis and subsequent equilibrium. In the light-activated chromatophore system, tests can be carried out over a wide range of driving forces by changing ambient redox potential and pH prior to activation. Here, two ambient redox potential poises were examined over a wide range of pH. (1) Low redox potential conditions set the Q pool half-reduced prior to activation. This potential establishes substrate QH_2 in or close to the Q_o site and essentially removes rate-limiting diffusion and exchange with the Q_o site. This initial condition also strongly favors the net oxidation of QH_2 and the reduction of the c- and b-chain components in re-equilibration after flash activation. (2) High redox potential conditions set the Q pool essentially fully oxidized. This potential requires QH_2 to be generated by the light-activated reaction center Q_B site and then to diffuse through a Q pool dominated by Q before exchanging with the Q_o site. This becomes a rate-limiting step in the overall process. These two initial conditions offer two distinctly different views of the Q_o site-mediated re-equilibration after activation that can be easily measured by the level of heme b_H reduction. By varying pH from 5 to 10, we can systematically examine changes in the driving force and the influence of any redox-coupled proton exchanges associated with side chains, oxidized FeS (p*K* ∼8), or reduced heme b_L (p*K* ∼9).

Figure 8 shows the yields of reduced heme b_H generated after a single flash. In the wild type, the yields follow the expectations from the calculated equilibrium over the pH 5−10 range for both initial redox poises (*5*). With the Q pool initially containing substrate QH_2 (Figure 8A), the yield of reduced heme b_H diminishes at pH values below 6 and above 9 (*5*). With the Q pool initially oxidized (Figure 8B), as the pH is lowered, the yield starts to diminish at higher pH values as expected from the diminished overall driving force (*5*). Figure 8 compares the wild type with the mutant E295V. The loss of the carboxyl function has essentially no effect on the equilibrium redox distributions between the Q pool and the *c*- and *b*-chains. Even in the particularly sensitive region of partial heme b_H reduction at the lower pH values, the pH/yield profiles of wild type and E295V are essentially the same.

These results indicate that Glu-295 does not influence the E_m values of any c- and b-chain component up to the 100 ms time scale of the measurements. The lack of effect in the wild type and the E295V mutant over such a broad range of initial poises of pH and redox conditions that encompass p*K* values of the oxidized FeS center, the reduced p*K* value

Table 1: Rates of Flash-Induced Heme b_H Reduction in the Wild Type and Glu-295 Mutants at pH 7

	QH_2		Q	
mutation	rate (s^{-1})	relative rate (% of wt)	rate (s^{-1})	relative rate (% of wt)
WT	**1092**	**100**	**64**	**100**
E295V	190	17	11	17
E295H	136	12	10	16
E295K	70	6	9	14
E295A	88	8	11	17
E295F	69	6		
E295Q	20	2	4	6

Table 2: Rates of Flash-Induced Heme b_H Reduction in the Wild Type (Bold, s^{-1}) and the Relative Rates in Glu-295 Mutants (% of Wild-Type)

	pH 5.1		pH 6		pH 7		pH 8		pH 9		pH 10	
mutation	QH_2	Q	QH_2	Q	QH_2	Q	QH_2	Q	QH_2	Q	QH_2	Q
WT	**72**		**358**	**54**	**1092**	**64**	**1460**	**101**	**2010**	**108**	**1434**	**87**
E295V	21		16	20	17	17	12		12	21	13	15
E295H			12		12	16			40	29	38	
E295K	17		6	11	6	14	20	31	26	37	24	18
E295A					8	17			10	10		
E295F					6							
E295Q	24		5	5	2	6	7		6	9	4	7

of heme b_L and both oxidized and reduced p*K* values of heme b_H rules against any significant change in the thermodynamics of the chains on mutation of Glu-295. This is consistent with the conclusions from experiments of Figures 2−7 that show no significant physical/chemical interacting partnerships of Glu-295 with either the FeS center or heme b_L. This view apparently extends to the other cofactors in the chains, cytochrome c_1, and heme b_H. Of course, an essential residue can have an effect only on reaction transition states and not on the equilibrium properties of the reactants and products; this requires an examination of kinetic measurements.

Effect of Glu-295 Mutation on the Time Scales of QH_2/Q Oxidation−Reduction Catalysis in the Q_o Site. Catalysis has kinetic barriers associated with substrate binding and release as well as those associated more directly with catalytic transitions states. The ability to observe kinetics under conditions of high and low concentrations of QH_2 substrate simply by changing the redox poise of the quinone pool helps to separate the possible effects on binding dynamics from those that are more closely linked to catalytic transition states. Glu-295 is likely to play an important role in QH_2/Q exchange and binding at Q_o if mutants minimally affect catalytic rates at low redox poise (where QH_2 is already present at Q_o before flash delivery of oxidants to start catalysis) but make conspicuous rate changes at high redox poise (where Q is present at the Q_o site and must be displaced to start catalysis upon flash delivery of QH_2 from the reaction center). However, if both rates are affected equally by mutations, then Glu-295 is more likely to be influential in steps of catalysis after quinone exchange and binding.

In Figure 9, the time-course of flash-induced heme b_H reduction was followed in the wild type and selected mutants when reduced substrate QH_2 was present in the Q_o site prior to flash activation or when QH_2 arrival at the Q_o site was delayed by diffusion. With QH_2 initially present in the Q_o site (Figure 9A, black), the rate of heme b_H reduction in E295V is slowed about 5-fold, whereas E295Q is slowed about 50-fold relative to the wild-type. In the absence of any inhibitor, the reduction of hemes *b* and their subsequent oxidation by the Q_i site takes place effectively in the millisecond time domain (Figure 9A, gray). Table 1 summarizes the rates and the degree of slowing displayed by all Glu-295 mutants under the same conditions at pH 7.0.

Figure 9B presents parallel results obtained when product oxidized Q is initially present in the Q_o site at the time of activation. Hydroquinone oxidation is slowed in the wild type, and most of the mutants show a similar percentage of slowing relative to the wild type under these oxidizing conditions as they showed under reducing conditions (Table 1).

The relative slowing effects of Val, Lys, Ala, and His are remarkably similar, considering the markedly different side chain characters that replace the Glu-295 carboxyl function. E295Q, which has the most dramatic inhibition, shows less contrast in the rate between high and low potential conditions, perhaps because Gln introduces structural changes at the site that impede catalysis even though Glu to Gln is a conservative volume change. When added to the minimal effects on the Q occupancy by EPR, the parallel rate effects of most mutants at high and low substrate QH_2 concentrations rules against wild-type Glu-295 playing a unique role in substrate quinone or hydroquinone binding and exchange.

One of the catalytic roles often suggested for Glu-295 is that of accepting and donating protons to quinone and the hydroquinone substrate (*11*, *13*, *22*−*24*). Indeed, the slowing of hydroquinone oxidation below pH 7 under optimal conditions has been suggested to reflect at least in part the protonation of this Glu at low pH (*11*, *26*), although others suggest that it is mostly due to the protonation of the FeS cluster histidine, which also takes a quinone proton (*69*−*71*). If Glu-295 were to play a specific, irreplaceable role in rate-limiting Q_o site proton exchange, then we may expect the wild-type pH profile (*5*) to be conspicuously altered by mutation. However, if the rate at each pH is affected equally by mutations and the same pH dependence of the rate slowing is maintained, then we may suspect that Glu-295 itself does not have a unique rate-limiting proton exchange role responsible for the pH rate dependence.

Figure 10 and Table 2 illustrate the rate of flash-induced heme b_H reduction in wild type and all Glu-295 mutants when reduced QH_2 or oxidized Q was present in the Q_o site at the time of activation over the pH range from 5 to 10. With reduced QH_2 present (Figure 10A), the wild type displays a smooth characteristic overall ∼15-fold change of rate as the pH is decreased. With oxidized Q present at the time of the flash (Figure 10B), the effect of pH on the rate is much less. The general effect upon loss of the carboxyl in the mutants is the systematic slowing down of the rates, although some mutants show a delay in the leveling-off of the rate at higher pH. If we were to classify these results in terms of possible p*K* shifts, then the His and Lys mutants appear to have a p*K* shifted to higher pH, whereas the Val mutant appears to have the same p*K* as that of wild-type Glu. Once again, Gln, with the slowest rates, has the most deviant behavior with what might be described as two p*K* values. pH dependences of wild-type and mutant rates at low redox potential are difficult to interpret but could be related to p*K* values of protonatable

residues, with the possible contribution of wild-type Glu and mutant Val obscured by a dominating p*K* effect of the FeS His, whereas p*K* values of Lys and His at position 295 dominate the effect of the FeS His.

DISCUSSION

The scale and character of the observed effects of Glu-295 mutants analyzed here under a very broad set of experimental conditions consistently indicate that the Q_o site can accommodate substantial structural changes at this position without impacting photosynthetic growth rates, without interfering with cytochrome bc_1 assembly, without significantly affecting the equilibrium properties of substrate occupancy of the Q_o site, and without noticeably affecting any of the equilibrium oxidation−reduction and coupled proton-release binding properties of the FeS, Q, and heme b_L redox partners. The remarkable absence of the effects of replacement of the carboxyl function of Glu-295 with aliphatic, aromatic, and base groups prompts comment on some of the roles ascribed to Glu 295. For instance, it seems difficult to envisage how a hydrophobic Val or basic Lys can play the same role as acidic Glu in accepting a proton from semiquinone bound in the Q_o site and in allowing, through the rotation of its own side-chain, the semiquinone anion to rotate from the FeS-proximal to the heme b_L-proximal position (*13*, *22*). Also, the observation that an H-bond between Glu-295 is not required for quinone binding and does not change the discrimination between oxidized and reduced quinone binding strength, makes it more difficult for such a bond to act as a catalytic gate that turns on or turns off binding depending on the redox states of FeS, heme b_L, and quinone (*10*, *25*). Likewise, the absence of any effect of Glu-295 removal on the E_m and pK_{red} values of heme b_L argues against any mechanism that relies on redox and proton-coupled charge interactions between heme b_L and Glu-295 (*11*, *18*, *23*). Furthermore, FTIR indicates that Glu-295 is not the principle carboxylic acid residue that is responsive to the redox changes in heme b_L. Instead, another as yet unidentified group appears to provide the charge compensating redox-linked protonation site linked to heme b_L oxidation−reduction and contributes to the pK_{red} 9 and pK_{ox} <5 on heme b_L revealed by potentiometry. This strong coupling will tend to diminish any long-range electrostatic coupling of heme b_L with other components of the Q_o site.

Even though the Glu-295 mutation consistently slows the optimal Q_o site catalytic rates within a range similar to the 2−50-fold observed in the related bacterial species *Rb. sphaeroides* (*22*, *34*) and the 2−5-fold seen in photosynthetic cytochrome b_6f (*35*, *36*), it appears to be neither essential nor have an irreplaceable role in Q_o site catalyzed two-electron oxidation−reduction and two-proton exchange with the external aqueous phase. This leaves us with no direct experimental information that can convincingly assign a role for Glu-295 in wild-type catalysis and proton management.

Q_o Site Resilience. The fact that the Q_o site can tolerate elimination of its carboxyl group and still support significant rates of hydroquinone oxidation suggests that the site is resilient (*30*, *31*) and that any role played by the acid group can be largely taken over by other residues or water molecules. A similar resiliency is seen in the Q_B site of reaction centers, where multiple protonatable residues share the task of proton management (reviewed in refs 72 and 73 (*72*, *73*)). In the Q_o site, such resiliency may be fostered by the conspicuous structural flexibility of the site that includes the large scale movement of one wall of the Q_o site as the FeS head domain swings away more than 10 Å and back again on the time scale of turnover and the related movement of the loop regions of cytochrome *b* (*9*, *57*, *74*, *75*). During this movement, the site is likely to be flooded with water molecules, which may well be part of a redundant network of hydrogen bond and proton donor/acceptors indicated by our experiments. Q_o site resiliency is also evident in other residues that share the same mutational pattern, that is, slow hydroquinone oxidation without impact on Q_o site quinone/hydroquinone binding and exchange (*51*, *76*). One of these is Tyr-147 of *Rba. capsulatus* cytochrome bc_1 (*76*) only a few Å apart from Glu-295 (Figure 11A) and also part of the cavity wall accommodating Q_o site inhibitors (Figure 11B). Certain mutants at other Q_o site positions also display a slowing without evidence of weakened substrate binding as distinct from side chains observed to slow catalysis by directly weakening quinone binding (Figure 11C and D and see also ref (*77*)).

Further evidence of resilience in the Q_o site is uncovered by inhibitors such as diphenylamine (DPA) that repeat the pattern of moderately slowing catalysis without displacing quinone. DPA titrations slow the catalytic mechanism (K_i 35 μM) by at least 10-fold before evidence of the elimination of substrate quinone/hydroquinone is observed (*58*). The related benzophenone (K_i 130 μM) has the same effect (Sharp, R. E., and Dutton, P. L., unpublished results). At this stage, we cannot identify the nature of the catalytic barriers raised by the exchange of the Glu-295 carboxylate or Tyr-147 hydroxyl to aliphatic, aromatic, amines, and amide, or upon introduction of the noncompetitive inhibitors diphenylamine or benzophenone, but it may be reasonable to consider that the degree of mutational slowing may be correlated with the degree of disruption of nonpolar/polar patterns or significant H-bonded water molecules in the site, which in the wild type support millisecond hydroquinone−quinone oxidation−reduction. This view offers a simple basis for the observed absence of effects of replacement of Glu-295 on Q_o site binding, redox, and coupled acid−base properties and for the observed resilience in electron-transferring and proton-exchanging catalysis. It is difficult to reconcile the demonstrated resilience with a crucial role of Glu-295 as that role becomes more critical and ultimately unique in many proposed models.

Defensive Catalysis in the Q_o Site? The traditional biochemical view of catalytic sites emphasizes the ability of protein to dramatically lower transition state barriers and speed the reaction by many orders of magnitude compared to the conventional reference rate of the reaction in aqueous solution. This viewpoint may not hold for hydroquinone oxidation and quinone reduction in the Q_o site. Indeed, relatively low barriers to catalysis in a watery site may be the basis of the observed resilience. The polarity of a watery environment supports the intermediate redox and protonation states in quinone oxidation and reduction (*78*−*80*). Two electron-two proton hydroquinone−quinone oxidation and reduction in aqueous solution at an electrode surface that provides a source or sink for electrons (*37*−*39*, *81*, *82*) can be as fast as 500 s^{-1}, only about two times slower than the

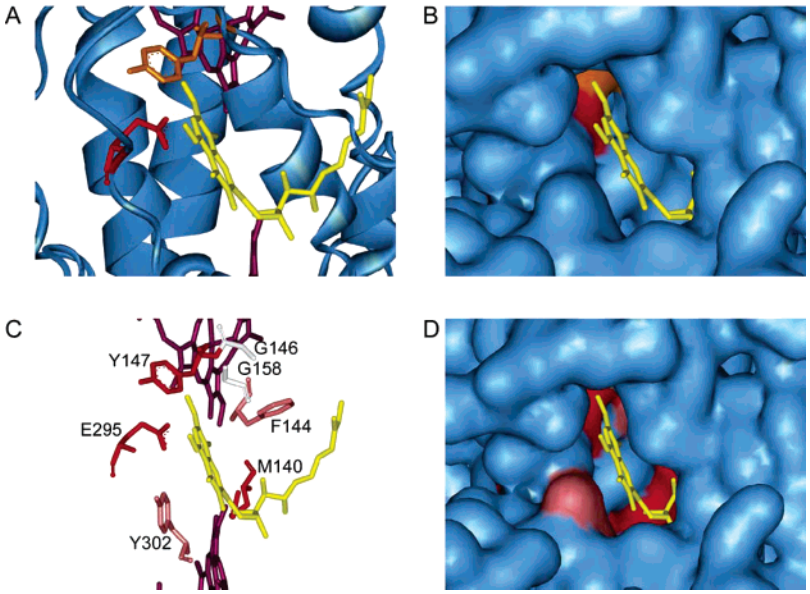

FIGURE 11: Sections of cytochrome *b* from the crystal structure of *Rba. capsulatus* cytochrome bc_1 (*19*). (A) Closely positioned side chains of E295 (red) and Y147 (orange) are shown on the background of a ribbon of cytochrome *b* (blue) with stigmatellin (yellow) and hemes (violet). (B) Molecular surface showing the inhibitor binding cavity with E295 (red) and Y147 (orange) components. The cavity is viewed from the side of the FeS cluster. Orientation of cytochrome *b* is the same as that in A. (C) Simplified map of the effects of mutating selected side chains in the Q_o site. Red corresponds to positions for which the mutated forms display kinetic inhibition without changing the occupancy of the Q_o site: E295 ((*22*) and this work), Y147 (*76*), and M140 (*51*). White corresponds to positions for which the mutated forms display kinetic inhibition and change the occupancy of the Q_o site: G146 (*64*), and G158 (*51*, *86*). Pink shows positions for which the mutated forms display mixed effects of red and white described above: F144 (*51*, *86*) and Y302 ((*87*, *88*); Daldal, F. et al., personal communication). Orientation of cytochrome *b* is similar to that shown in A and B. (D) Molecular surface showing the inhibitor binding cavity and residues depicted in C. Orientation of cytochrome *b* and color codes are the same as those in C.

maximum turnover of the Q_o site. Thus, once redox partners FeS and heme b_L are placed within ~14 Å and, hence, in rapid electron tunneling distance of substrate quinone, oxidation−reduction may be naturally rapid in a sufficiently water-like environment. There is some evidence that reaction coordinates for hydroquinone oxidation may be similar in protein and nonprotein biomimetic electron-transfer systems (*83*). The role of natural selection in the engineering of the Q_o site may not be to lower catalytic barriers but to raise barriers specifically against certain energy wasting short circuit reactions (*5*, *6*).

Although the nature of the barriers that prevent short circuits in the Q_o site remains unknown, the specific introduction of barriers may be general in respiratory and photosynthetic quinone sites. For instance, the semiquinone formed in the Q_A and Q_B sites of reaction centers and the Q_i site of cytochrome bc_1 are all held as unprotonated anions (*73*, *84*). Recent work on the Q_A site (*85*) indicates that neutral quinone species rapidly enter and leave the site, whereas anionic quinones are slow. This prompts the suggestion that these quinone sites may raise barriers to impede protonation of the semiquinone anion in order to avoid premature and deleterious loss of the neutral semiquinone from the site. In cytochrome bc_1, the analogous barrier would impede semiquinone formation in certain short-circuit prone redox states of FeS and heme b_L. Thus, rather than using mutagenesis to target residues that may *lower* catalytic barriers to quinone oxidation and reduction, it may be more revealing of the engineering of cytochrome bc_1 to search for residues that *raise* barriers against counterproductive electron or proton transfer. These Q_o site mutants would have the unusual signature of speeding up short-circuit reactions rather than slowing down the physiological reactions. Whether this might be accomplished by altering quinone binding or slowing electron transfer to/from bound quinone remains to be seen.

ACKNOWLEDGMENT

We thank Professor Fevzi Daldal for providing us with a cytochrome bc_1 mutagenesis and expression system in *Rba. capsulatus* and for helpful discussions throughout the course of this work.

REFERENCES

1. Berry, E. A., Guergova-Kuras, M., Huang, L., and Crofts, A. R. (2000) Structure and function of cytochrome *bc* complexes, *Annu. Rev. Biochem. 69*, 1005−1075.
2. Darrouzet, E., Cooley, J. W., and Daldal, F. (2004) The cytochrome bc_1 complex and its homologue the b_6f complex: similarities and differences, *Photosynth. Res. 79*, 25−44.
3. Allen, F. J. (2004) Cytochrome b_6f: structure for signalling and vectorial metabolism, *Trends Plant Sci. 9*, 130−137.
4. Cooley, J. W., Darrouzet, E., and Daldal, F. (2004) Bacterial Hydroquinone:Cytochrome c Oxidoreductases: Physiology, Structure, and Function, in *Respiration in Archaea and Bacteria* (Zannoni, D., Ed.), Kluwer Academic Publishers, Norwell, MA.
5. Osyczka, A., Moser, C. C., Daldal, F., and Dutton, P. L. (2004) Reversible redox energy coupling in electron-transfer chains, *Nature 427*, 607−612.
6. Osyczka, A., Moser, C. C., and Dutton, P. L. (2005) Fixing the Q cycle, *Trends Biochem. Sci. 30*, 176−182.
7. Kramer, D. M., Roberts, A. G., Muller, F., Cape, J., and Bowman, M. K. (2004) Q-cycle bypass reactions at the Q_o site of cytochrome bc_1 (and related) complexes, *Methods Enzymol. 382*, 21−45.
8. Muller, F., Crofts, A. R., and Kramer, D. M. (2002) Multiple Q-cycle bypass reactions at the Q_o site of the cytochrome bc_1 complex, *Biochemistry 41*, 7866−7874.
9. Darrouzet, E., Moser, C. C., Dutton, P. L., and Daldal, F. (2001) Large scale domain movement in cytochrome bc_1: a new device for electron transfer in proteins, *Trends Biochem. Sci. 26*, 445−451.

10. Rich, P. R. (2004) The quinone chemistry of *bc* complexes, *Biochim. Biophys. Acta 1658*, 165−171.
11. Mulkidjanian, A. Y. (2005) Ubiquinol oxidation in the cytochrome bc_1 complex: reaction mechanism and prevention of short-circuiting, *Biochim. Biophys. Acta 1709*, 5−34.
12. Berry, E. A., and Huang, L.-S. (2003) Observations concerning the quinol oxidation site of the cytochrome bc_1 complex, *FEBS Lett. 555*, 13−20.
13. Crofts, A. R., Barquera, B., Gennis, R. B., Kuras, R., Guergova-Kuras, M., and Berry, E. A. (1999) Mechanism of ubiquinol oxidation by the bc_1 complex: different domains of the quinol binding pocket and their role in the mechanism and binding of inhibitors, *Biochemistry 38*, 15807−15826.
14. Cape, J. L., Strahan, J. R., Lenaeus, M. J., Yuknis, B. A., Le, T. T., Shepherd, J. N., Bowman, M. K., and Kramer, D. M. (2005) The respiratory substrate rhodoquinol induces Q-cycle bypass reactions in the yeast cytochrome bc_1 complex. Mechanistic and physiological implications, *J. Biol. Chem. 280*, 34654−34660.
15. Xia, D., Yu, C. A., Kim, H., Xia, J. Z., Kachurin, A. M., Zhang, L., Yu, L., and Deisenhofer, J. (1997) Crystal structure of the cytochrome bc_1 complex from bovine heart mitochondria, *Science 277*, 60−66.
16. Iwata, S., Lee, J. W., Okada, K., Lee, J. K., Iwata, M., Rasmussen, B., Link, T. A., Ramaswamy, S., and Jap, B. K. (1998) Complete structure of the 11-subunit bovine mitochondrial cytochrome bc_1 complex, *Science 281*, 64−71.
17. Zhang, Z., Huang, L., Shulmeister, V. M., Chi, Y. I., Kim, K. K., Hung, L. W., Crofts, A. R., Berry, E. A., and Kim, S. H. (1998) Electron transfer by domain movement in cytochrome bc_1, *Nature 392*, 677−684.
18. Hunte, C., Koepke, J., Lange, C., Robmanith, T., and Michel, H. (2000) Structure at 2.3 Å resolution of the cytochrome bc_1 complex from the yeast *Saccharomyces cerevisiae* co-crystalized with an antibody F_v fragment, *Structure 8*, 669−684.
19. Berry, E. A., Huang, L.-S., Saechao, L. K., Pon, N. G., Valkova-Valchanova, M. B., and Daldal, F. (2004) X-ray structure of *Rhodobacter capsulatus* cytochrome bc_1: comparison with its mitochondrial and chloroplast counterparts, *Photosynth. Res. 81*, 251−275.
20. Stroebel, D., Choquet, Y., Popot, J.-L., and Picot, D. (2003) An atypical haem in the cytochrome b_6f complex, *Nature 426*, 413−418.
21. Kurisu, G., Zhang, H., Smith, J. L., and Cramer, W. A. (2003) Structure of the cytochrome b_6f complex of oxygenic photosynthesis: tuning the cavity, *Science 302*, 1009−1014.
22. Crofts, A. R., Hong, S., Ugulava, N. B., Barquera, B., Gennis, R., Guergova-Kuras, M., and Berry, E. A. (1999) Pathways for proton release during ubihydroquinone oxidation by the bc_1 complex, *Proc. Natl. Acad. Sci. U.S.A. 96*, 10021−10026.
23. Hunte, C., Palsdottir, H., and Trumpower, B. L. (2003) Protonmotive pathways and mechanisms in the cytochrome bc_1 complex, *FEBS Lett. 545*, 39−46.
24. Palsdottir, H., Lojero, C. G., Trumpower, B. L., and Hunte, C. (2003) Structure of the yeast cytochrome bc_1 complex with a hydroxyquinone anion Q_o site inhibitor bound, *J. Biol. Chem. 278*, 31303−31311.
25. Trumpower, B. L. (2002) A concerted, alternating sites mechanism of ubiquinol oxidation by the dimeric cytochrome bc_1 complex, *Biochim. Biophys. Acta 1555*, 166−173.
26. Covian, R., and Moreno-Sanchez, R. (2001) Role of protonatable groups of bovine heart bc_1 complex in ubiquinol binding and oxidation, *Eur. J. Biochem, 268*, 5783−5790.
27. Muller, F. L., Roberts, A. G., Bowman, M. K., and Kramer, D. M. (2003) Architecture of the Q_o site of the cytochrome bc_1 complex probed by superoxide production, *Biochemistry 42*, 6493−6499.
28. Brasseur, G., Bruscella, P., Bennefoy, V., and Lemesle-Meunier, D. (2002) The bc_1 complex of the iron-grown acidophilic chemolithotrophic bacterium *Acidithiobacillus ferrooxidans* functions in the reverse but not in the forward direction. Is there a second bc_1 complex? *Biochim. Biophys. Acta 1555*, 37−43.
29. Schutz, M., Brugna, M., Lebrun, E., Baymann, F., Huber, R., Stetter, K.-O., Hauska, G., Toci, R., Lemesle-Meunier, D., Tron, P., Schmidt, C., and Nitschke, W. (2000) Early evolution of cytochrome *bc* complexes, *J. Mol. Biol. 300*, 663−675.
30. Kraut, D. A., Carroll, K. S., and Herschlag, D. (2003) Challenges in enzyme mechanism and energetics, *Annu. Rev. Biochem. 72*, 517−571.
31. Peracchi, A. (2001) Enzyme catalysis: removing chemically 'essential' residues by site-directed mutagenesis, *Trends Biochem. Sci. 26*, 497−503.
32. Knowles, J. M. (1991) Enzyme catalysis: not different, just better, *Nature 350*, 121−124.
33. Stehlin, C., Heacock II, D. H., Liu, H., and Musier-Forsyth, K. (1997) Chemical modification and site-directed mutagenesis of the single cysteine in motif 3 of class II *Escherichia coli* prolyl-tRNA synthetase, *Biochemistry 36*, 2932−2938.
34. Crofts, A. R., Hacker, B., Barquera, B., Yu, C. H., and Gennis, R. (1992) Structure and function of the *bc*-complex of *Rhodobacter sphaeroides*, *Biochim. Biophys. Acta 1101*, 162−165.
35. Zito, F., Finazzi, G., Joliot, P., and Wollman, F.-A. (1998) Glu78, from the conserved PEWY sequence of subunit IV, has a key function in cytochrome b_6f turnover, *Biochemistry 37*, 10395−10403.
36. Finazzi, G. (2002) Redox-coupled proton pumping activity in cytochrome b_6f, as evidenced by the pH dependence of electron transfer in whole cells of *Chlamydomonas reinhardtii*, *Biochemistry 41*, 7475−7482.
37. Forster, R. J., and O'Kelly, J. P. (2001) Protonation reactions of anthraquinone-2, 7-disulphonic acid in solution and within monolayers, *J. Electroanal. Chem. 498*, 127−135.
38. Hong, H.-G., and Park, W. (2001) Electrochemical characteristics of hydroquinone-terminated self-assembled monolayers on gold, *Langmuir 17*, 2485−2492.
39. Budavari, V., Szucs, A., Oszko, A., and Novak, M. (2003) Formation and electrochemical behavior of self-assembled multilayers involving quinone, *Electrochim. Acta 48*, 3499−3508.
40. Atta-Asafo-Adjei, E., and Daldal, F. (1991) Size of the amino acid side chain at position 158 of cytochrome *b* is critical for an active cytochrome bc_1 complex and for photosynthetic growth of *Rhodobacter capsulatus*, *Proc. Natl. Acad. Sci. U.S.A. 88*, 492−496.
41. Valkova-Valchanova, M. B., Saribas, A. S., Gibney, B. R., Dutton, P. L., and Daldal, F. (1998) Isolation and characterization of a two-subunit cytochrome b-c_1 subcomplex from *Rhodobacter capsulatus* and reconstitution of its ubihydroquionone oxidation (Q_o) site with purified Fe-S protein subunit, *Biochemistry 37*, 16242−16251.
42. Osyczka, A., Dutton, P. L., Moser, C. C., Darrouzet, E., and Daldal, F. (2001) Controlling the functionality of cytochrome c_1 redox potentials in the *Rhodobacter capsulatus* cytochrome bc_1 complex through disulfide anchoring of a loop and a β-branched amino acid near the heme-ligating methionine, *Biochemistry 40*, 14547−14556.
43. Dutton, P. L. (1978) Redox potentiometry: determination of midpoint potentials of oxidation−reduction components of biological electron-transfer systems, *Methods Enzymol. 54*, 411−435.
44. Iwaki, M., Puustinen, A., Wikstrom, M., and Rich, P. R. (2003) ATR-FTIR spectroscopy of the P_M and F intermediates of bovine and *Paracoccus denitrificans* cytochrome *c* oxidase, *Biochemistry 42*, 8809−8817.
45. Iwaki, M., Osyczka, A., Moser, C. C., Dutton, P. L., and Rich, P. R. (2004) ATR-FTIR spectroscopy studies of iron−sulfur protein and cytochrome c_1 in the *Rhodobacter capsulatus* cytochrome bc_1 complex, *Biochemistry 43*, 9477−9486.
46. Iwaki, M., Yakovlev, G., Hirst, J., Osyczka, A., Dutton, P. L., Marshall, D., and Rich, P. R. (2005) Direct observation of redox-linked histidine protonation changes in the iron−sulfur protein of cytochrome bc_1 complex by ATR-FTIR spectroscopy, *Biochemistry 44*, 4230−4237.
47. Robertson, D. E., Davidson, E., Prince, R. C., van der Berg, W. H., Marrs, B. L., and Dutton, P. L. (1986) Discrete catalytic sites for quinone in the ubiquinol-cytochrome c_2 oxidoreductase of *Rhodopseudomonas capsulata*, *J. Biol. Chem. 261*, 584−591.
48. Sharp, R. E., Palmitessa, A., Gibney, B. R., Daldal, F., Moser, C. C., and Dutton, P. L. (1999) Correlation between Cytochrome bc_1 Structure and Function. Spectroscopic and Kinetic Observations on Q_o Site Occupancy and Dynamics, in *The Phototrophic Prokaryotes* (Peschek, G. A., Loffelhard, W., and Schmetterer, G., Eds.), Kluwer Academic, Plenum Publishers, NY.
49. Ding, H., Robertson, D. E., Daldal, F., and Dutton, P. L. (1992) Cytochrome bc_1 complex [2Fe-2S] cluster and its interaction with ubiquinone and ubihydroquinone at the Q_o site: a double-occupancy Q_o site model, *Biochemistry 31*, 3144−3158.
50. Ding, H., Moser, C. C., Robertson, D. E., Tokito, M. K., Daldal, F., and Dutton, P. L. (1995) Ubiquinone pair in the Q_o site central

to the primary energy conversion reactions of cytochrome bc_1 complex, *Biochemistry 34*, 15979−15996.
51. Ding, H., Daldal, F., and Dutton, P. L. (1995) Ion pair formation between basic residues at 144 of cyt *b* polypeptide and the ubiquinones at the Q_o site of the cyt bc_1 complex, *Biochemistry 34*, 15997−16003.
52. von Jagow, G., and Link, T. A. (1986) Use of specific inhibitors on the mitochondrial bc_1 complex, *Methods Enzymol. 126*, 253−271.
53. Brandt, U., Haase, U., Schagger, H., and von Jagov, G. (1991) Significance of the "Rieske" iron−sulfur protein for formation and function of the ubiquinol-oxidation pocket of mitochondrial cytochrome *c* reductase (bc_1 complex), *J. Biol. Chem. 266*, 19958−19964.
54. von Jagov, G., and Ohnishi, T. (1985) The chromone inhibitor stigmatellin: binding to the ubiquinol oxidation center at the C-side of the mitochondrial membrane, *FEBS Lett. 185*, 311−315.
55. Bowyer, J. R., Dutton, P. L., Prince, R. C., and Crofts, A. R. (1980) The role of the Rieske iron−sulfur center as the electron donor to ferricytochrome c_2 in *Rhodopseudomonas sphaeroides*, *Biochim. Biophys. Acta 592*, 445−460.
56. Matsuura, K., Bowyer, J. R., Ohnishi, T., and Dutton, P. L. (1983) Inhibition of electron transfer by 3-alkyl-2-hydroxy-1,4-naphthoquinones in the ubiquinol-cytochrome *c* oxidoreductases of *Rhodopseudomonas sphaeroides* and mammalian mitochondria, *J. Biol. Chem. 258*, 1571−1579.
57. Darrouzet, E., Valkova-Valchanova, M. B., and Daldal, F. (2002) The [2Fe-2S] cluster E_m as an indicator of the iron−sulfur subunit position in the ubihydroquinone oxidation site of the cytochrome bc_1 complex, *J. Biol. Chem. 2002*, 3464−3470.
58. Sharp, R. E., Palmitessa, A., Gibney, B. R., White, J. L., Moser, C. C., Daldal, F., and Dutton, P. L. (1999) Ubiquinone binding capacity of the *Rhodobacter capsulatus* cytochrome bc_1 complex: effect of diphenylamine, a weak binding Q_o site inhibitor, *Biochemistry 38*, 3440−3446.
59. Sharp, R. E., Gibney, B. R., Palmitessa, A., White, J. L., Dixon, J. A., Moser, C. C., Daldal, F., and Dutton, P. L. (1999) Effect of inhibitors on the ubiquinone binding capacity of the primary energy conversion site in the *Rhodobacter capsulatus* cytochrome bc_1 complex, *Biochemistry 38*, 14973−14980.
60. Darrouzet, E., Valkova-Valchanova, M. B., Moser, C. C., Dutton, P. L., and Daldal, F. (2000) Uncovering the [2Fe2S] domain movement in cytochrome bc_1 and its implications for energy conversion, *Proc. Natl. Acad. Sci. U.S.A. 97*, 4567−4572.
61. Darrouzet, E., Valkova-Valchanova, M. B., and Daldal, F. (2000) Probing the role of the Fe−S subunit hinge region during Q_o site catalysis in *Rhodobacter capsulatus* bc_1 complex, *Biochemistry 39*, 15475−15483.
62. Cooley, J. W., Roberts, A. G., Bowman, M. K., Kramer, D. M., and Daldal, F. (2004) The raised midpoint potential of the [2Fe2S] cluster of cytochrome bc_1 is mediated by both the Q_o site occupants and the head domain position of the Fe−S protein subunit, *Biochemistry 43*, 2217−2227.
63. Salerno, J. C. (1984) Cytochrome electron spin resonance line shapes, ligand fields, and components stoichiometry in ubiquinol-cytochrome *c* oxidoreductase, *J. Biol. Chem. 259*, 2331−2336.
64. Saribas, A., Ding, H., Dutton, P. L., and Daldal, F. (1997) Substitutions at position 146 of cytochrome *b* affect drastically the properties of heme b_L and the Q_o site of *Rhodobacter capsulatus* cytochrome bc_1 complex, *Biochim. Biophys. Acta 1319*, 99−108.
65. Cooley, J. W., Ohnishi, T., and Daldal, F. (2005) Binding dynamics at the quinone reduction (Q_i) site influence the equilibrium interactions of the iron−sulfur protein and hydroquinone oxidation (Q_o) site of the cytochrome bc_1 complex, *Biochemistry 44*, 10520−10532.
66. Dervartanian, D. V., Albracht, S. P. J., Berden, J. A., van Gelder, B. F., and Slater, E. C. (1973) The EPR spectrum of isolated complex III, *Biochim. Biophys. Acta 292*, 496−501.
67. Barth, A. (2000) The infrared absorption of amino acid side chains, *Prog. Biophys. Mol. Biol. 74*, 141−173.
68. Rich, P. R., and Iwaki, M. (2005) Infrared Protein Spectroscopy as a Tool to Study Protonation Reactions within Proteins, in *Biophysical and Structural Aspects of Bioenergetics* (Wikstrom, M., Ed.) pp 314−333, Royal Society of Chemistry, Cambridge, U.K.
69. Brandt, U., and Okun, J. G. (1997) Role of deprotonation events in ubihydroquinone: cytochrome *c* oxidoreductase from bovine heart and yeast mitochondria, *Biochemistry 36*, 11234−11240.
70. Hong, S., Ugulava, N., Guergova-Kuras, M., and Crofts, A. R. (1999) The energy landscape for ubihydroquinone oxidation at the Q_o site of the bc_1 complex in *Rhodobacter sphaeroides*, *J. Biol. Chem. 274*, 33931−33944.
71. Ugulava, N. B., and Crofts, A. R. (1998) CD-monitored redox titration of the Rieske Fe-S protein of *Rhodobacter sphaeroides*: pH dependence of the midpoint potential in isolated bc_1 complex and in membranes, *FEBS Lett. 440*, 409−413.
72. Paddock, M. L., Feher, G., and Okamura, M. Y. (2003) Proton-transfer pathways and mechanism in bacterial reaction centers, *FEBS Lett. 555*, 45−50.
73. Wraight, C. A. (2004) Proton and electron transfer in the acceptor quinone complex of photosynthetic reaction centers from *Rhodobacter sphaeroides*, *Front. Biosci. 9*, 309−337.
74. Darrouzet, E., and Daldal, F. (2003) Protein−protein interactions between cytochrome *b* and the Fe−S protein subunits during QH_2 oxidation and large-scale domain movement in the bc_1 complex, *Biochemistry 42*, 1499−1507.
75. Darrouzet, E., and Daldal, F. (2002) Movement of the iron−sulfur subunit beyond the *ef* loop of cytochrome *b* is required for multiple turnovers of the bc_1 complex but not for single turnover Q_o site catalysis, *J. Biol. Chem. 277*, 3471−3476.
76. Saribas, A. S., Ding, H., Dutton, P. L., and Daldal, F. (1995) Tyrosine 147 of cytochrome *b* is required for efficient electron transfer at the ubihydroquinone oxidase site (Q_o) of the cytochrome bc_1 complex, *Biochemistry 34*, 16004−16012.
77. Crofts, A. R., and Berry, E. A. (1998) Structure and function of the cytochrome bc_1 complex of mitochondria and photosynthetic bacteria, *Curr. Opin. Struct. Biol. 8*, 501−509.
78. Rich, P. R. (1981) Electron-transfer reactions between quinols and quinones in aqueous and aprotic media, *Biochim. Biophys. Acta 637*, 28−33.
79. Rich, P. R. (1982) Electron and proton transfers in chemical and biological quinone systems, *Faraday Discuss. Chem. Soc. 74*, 349−364.
80. Rich, P. R., and Bendall, D. S. (1980) The kinetics and thermodynamics of the reduction of cytochrome *c* by substituted *p*-benzoquinols in solution, *Biochim. Biophys. Acta 592*, 506−518.
81. Katz, E., and Willner, I. (1997) Kinetic separation of amperometric responses of composite redox-active monolayers assembled onto Au electrodes: implications to the monolayers' structure and composition, *Langmuir 13*, 3364−3373.
82. Gordillo, G. J., and Schiffrin, D. J. (1994) Redox properties of ubiquionone (UQ_{10}) adsorbed on a mercury electrode, *J. Chem. Soc., Faraday Trans. 90*, 1913−1922.
83. Cape, J. L., Bowman, M. K., and Kramer, D. M. (2005) Reaction intermediates of quinol oxidation in a photoactivatable system that mimics electron transfer in the cytochrome bc_1 complex, *J. Am. Chem. Soc. 127*, 4208−4215.
84. Robertson, D. E., Prince, R. C., Bowyer, J. R., Matsuura, K., Dutton, P. L., and Ohnishi, T. (1984) Thermodynamic properties of the semiquinone and its binding site in the ubiquinol-cytochrome *c* (c_2) oxidoreductase of respiratory and photosynthetic systems, *J. Biol. Chem. 259*, 1758−1763.
85. Madeo, J., and Gunner, M. R. (2005) Modeling binding kinetics at the Q_A site in bacterial reaction centers, *Biochemistry 44*, 10994−11004.
86. Robertson, D. E., Daldal, F., and Dutton, P. L. (1990) Mutants of ubiquinol-cytochrome c_2 oxidoreductase resistant to Q_o site inhibitors: consequences for ubiquinone and ubiquinol affinity and catalysis, *Biochemistry 29*, 11249−11260.
87. Fisher, N., Castleden, C. K., Bourges, I., Brasseur, G., Dujardin, G., and Meunier, B. (2004) Human desease-related mutations in cytochrome *b* studied in yeast, *J. Biol. Chem. 279*, 12951−12958.
88. Mather, M. W., Darrouzet, E., Valkova-Valchanova, M. B., Cooley, J. W., McIntosh, M. T., Daldal, F., and Vaidya, A. B. (2005) Uncovering the molecular mode of action of the antimalarial drug atovaquone using a bacterial system, *J. Biol. Chem. 280*, 27458−27465.

BI060013A